To be published in EDP Science as Proceedings of the Tokyo LCWS 2024 Conference

The alignment of the accelerator modules of the Cool Copper Collider C^3 with the Rasnik 3-point alignment system

Harry van der Graaf[1,*], *Niels* van Bakel[1], *Bram* Bouwens[2], *Martin* Breidenbach[3], *Andrew* Haase[3], *Joris* van Heijningen[4], *Anoop Nagesh* Koushik[5], *Emilio* Nanni[3], *Tristan* du Pree[6], *Nick* van Remortel[5], and *Caterina* Vernieri[3]

[1]Nikhef, Science Park 105, 1098 XG Amsterdam, The Netherlands
[2]Amsterdam Scientific Instruments ASI, Science Park 106, Amsterdam, The Netherlands
[3]SLAC, Stanford, CA, USA
[4]VU, Amsterdam, The Netherlands
[5]University of Antwerp, Belgium
[6]Twente University, The Netherlands

Abstract. For C^3, some 2000 accelerator modules must be 5D positioned, within 10 μm transversal, on a 2.3 km long straight line, for both linacs. In the Rasnik alignment system, light from a point-like monochromatic source falls on a zone lens, forming a Fraunhofer diffraction pattern on an image pixel sensor. The alignment of three objects can be obtained by analyzing the position of the diffraction pattern on the sensor. The alignment of a large number of objects can be realized by fixing a stick on each object, carrying all three Rasnik components. With this leap frog geometry, all sticks are mutually coupled, forming a multipoint alignment system.
The system should operate in ambient air, in vacuum, and in liquid nitrogen. Due to the heat dissipation of these components, bubbles are formed, causing an error in the measured alignment when crossing the optical path. Various methods of beam shielding are presented. With the Quarter Cryo Module (QCM), essential studies will be carried out, enabling the realization of C^3. The QCM will be equipped with four Rasnik chains, measuring alignment parameters with redundancy. In addition, the bubble-induced vibrations of the accelerator components can be registered accurately.

1 Introduction

1.1 The Cool Copper Collider C^3

The Cool Copper Collider C^3 is a proposal for a linear collider with two high gradient accelerators each about 2.3 km long. The accelerators take electrons and positrons to 125 GeV (250 GeV center of mass) initially, and to 275 GeV (550 GeV center of mass) in a second stage with only adding RF power [1].

The key element of this accelerator is the 1-meter long *Accelerator Structure*. It is made of two copper half bars, both 3D milled, enabling full 3D control of the shape of RF cavities, see Figure 1. The higher accelerating gradient is possible due to improvements of the geometry

*e-mail: μvdgraaf@nikhef.nl

of the accelerating cavities in the Accelerator Structures, where special attention is paid to the RF couplers where the strongest electromagnetic fields occur. A further increase in the accelerating gradient results from lowering the operationing temperature to 80 K, being the boiling point of liquid nitrogen (LN_2) at a pressure of 2 bars. With the copper structures utilized in C^3, this enables a significant rise of the maximum applicable electric field (Fowler-Nordheim breakdown limit).

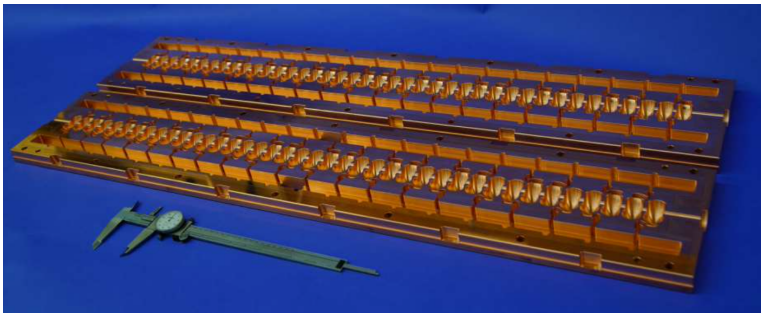

Figure 1: Both halves of the C^3 Accelerator Structure prior to braze. The one meter structure consists of 40 cavities. A RF manifold that runs parallel to the structure feeds 20 cavities on each side. The structure operates at 5.712 GHz.

The C^3 main linac will consist of accelerating units called CryoModules (CM): see Figure 2. Each cryomodule is an assembly of four "Rafts", each consisting of two Accelerator Structures and one Quad. A Quad is an adjustable field strength quadrupole made with permanent magnets, and includes a Beam Position Monitor (BPM), providing real time actual precision data of the 2D position of the beam.

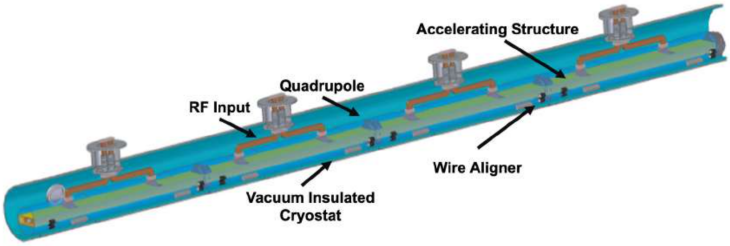

Figure 2: The 9 meter long CryoModule CM.

Proper operations of the electron and positron linacs, each consisting of 275 CryoModules, require accurate alignment over a length of 2.3 km, with a typical precision of 10 μm in both transversal directions, relative to components within 10 meters. At longer scales this tolerance can be relaxed further. This can be achieved by the Rasnik alignment system with its 2D spatial resolution of 5 nm/$\sqrt{Hz}$. With this sensitivity, the Rasnik data can be well employed, during the R&D phase, for studying bubble-induced motions of the accelerator components. Moreover, deformation of the linacs due to local seismic activity may require real time corrections, in particular at the mini-beta quadrupoles at the tips of the linacs[2].

1.2 The Rasnik 3-point alignment system

The first **R**ed **A**lignment **S**ystem **Nik**hef (Rasnik) was developed in 1983 for the alignment of the muon chambers in the Muon Spectrometer of the L3 experiment at CERN [3]. As optical sensors , 4-quadrant photodiodes were used. In 1993, CMOS image sensors became available, and Rasnik evolved into a system in which a back-illuminated coded mask is projected, by means of a positive singlet lens, onto the image sensor. Since 2005, 8000 of these Rasnik systems have been flawlessly operating in the ATLAS experiment at CERN. With these Rasnik systems, composed from low-cost, commercially available components, the 2D alignment of three points can be measured with a spatial resolution of 1 nm. The best *spatial resolution power* of 7 pm $\sqrt{\text{Hz}}$ was obtained with an image frame rate of 250 Hz [4].

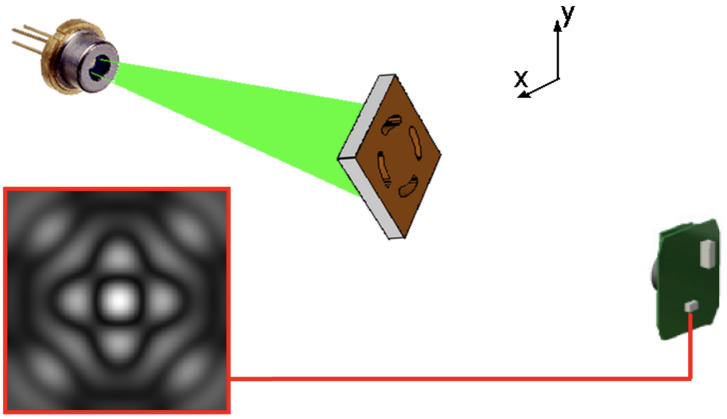

Figure 3: Principle of the RasDif system. The monochromatic waves, arriving at the zone lens, result in a diffraction pattern on the image sensor.

For the alignment of active beam elements of future CLIC and ILC linear colliders, systems with a span between the image sensor and the mask of a Rasnik system larger than 20 m are required. The diameter and focal length of the required lens become impractically large, and its replacement by a zone lens was considered [5, 6]. In the RasDif system, depicted in Figure 3, the back-illuminated coded mask is replaced by a monochromatic point-like light source generating spherical waves onto the zone lens. This results in a typical diffraction pattern onto the image sensor: the position of this pattern on the sensor is a measure for the 3-point alignment of light source, zone lens and image sensor, respectively. For C^3, this system will be applied since lenses cannot be used: a sharp image in air would result in a blurred image when the lens is submerged in LN_2 with higher index of refraction. In the following, we define a Rasnik system as the combination of a monochromatic light source, a zone lens and an image sensor.

1.3 The alignment of a multiple of objects with a multiple of Rasnik systems

The alignment of a series of multiple of objects is possible by means of *chain plates*, depicted in Figure 4. Each of the identical chain plates includes the three Rasnik components: a light source, a zone lens and an image sensor. The optical axes of the individual Rasnik systems are slightly tilted with respect to the common z-axis (beam direction).

The chain plates take the form of *sticks*, mounted onto Accelerator Structures. When two sticks are mounted on each Accelerator Structure, the relative position of an element, relative

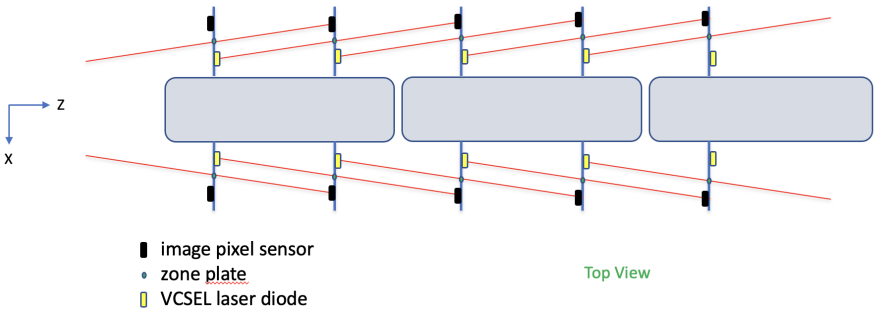

Figure 4: The 'leap frog' multipoint alignment system: with the known alignment of any set of three adjacent chain-plates, the alignment of all chain-plates is known.

to a neighbouring element, is known in 5 degrees of freedom. Note that the rather irrelevant position in z is not registered by Rasnik. By having chains at both sides of the Accelerator Structures, thus four on each element, the data is redundant, and its consistency is a measure for Rasnik's performance.

2 Operating Rasnik in Liquid Nitrogen at 80 K

A first condition is that the light source and image sensor operate in LN_2, in vacuum, and in ambient air at room temperature. Many electronic components fail in these conditions. A second condition is that the alignment measurements should not be affected by the medium. After the assembly of a CM, the alignment of the eight Accelerator Structures and four Quads can be adjusted and set while in ambient air. The measured change in alignment going to vacuum and, later, to LN_2 should only be due to actual changes in the positions of Accelerator Structures and Quads. As a consequence, the Rasnik light paths have to be independent of the index of refraction n of the ambient medium.

2.1 Operating the light source in LN_2

The light source has to be monochromatic and have a coherence length larger than the order one meter distance between light source and image sensor. In addition, the effective dimension of the source should be smaller than the smallest periodic pattern of the diffraction image on the image sensor, in order to be considered as point-like light source. Many low-cost laser diodes meet these specifications, and almost all of these have been found to be operational in LN_2, albeit that, in most cases, their operating voltage raised from 2 V to 5 V as the temperature decreases from room temperature to 80 K. Since the diode threshold voltage rises proportionally, care must be taken when the diode is switched on ('cold start'): a too large current may destroy the diode. Furthermore, no changes were observed in the typical elliptical divergent beam profile and in the efficiency of the laser diode (light power/current ratio).

In LN_2, the power dissipation of a laser diode causes bubble formation. These bubbles may pass the light output path of the diode, influencing the diffraction image on the image sensor, thus affecting the measurements of Rasnik X and Y. Various approaches have been tested to mitigate this effect. The first method places a *cow catcher* beneath the laser diode: see Figure 5. Another approach pursued was to glue a small glass bar onto the window of the

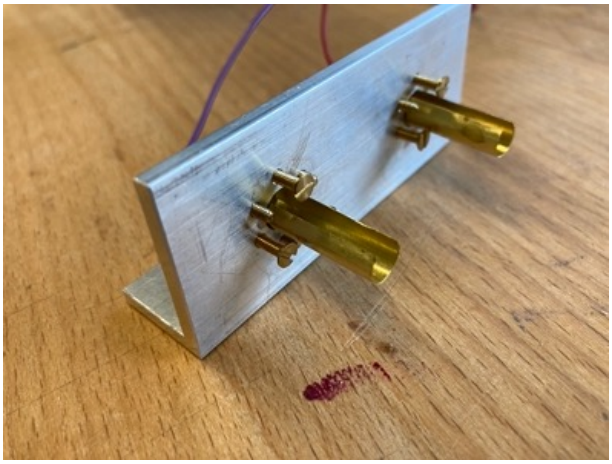

Figure 5: Cow catchers below front side of laser diodes, keeping self-generated bubbles out of the light path. Bubbles, potentially crossing the light path of the laser diode, are forced to go around.

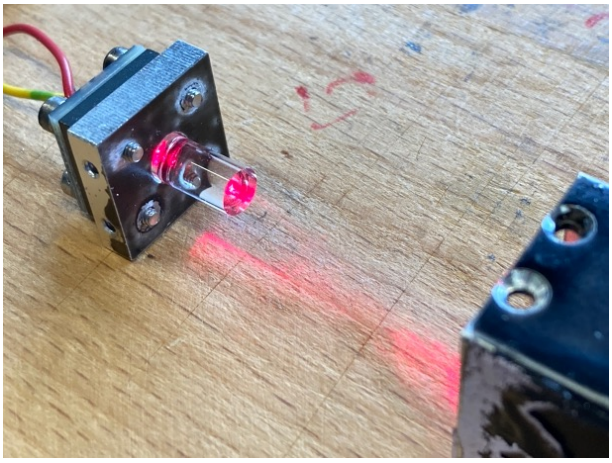

Figure 6: Glass rod, glued onto the window of a laser diode. Bubbles formed near the laser diode are unable to traverse the optical path.

laser diode, as shown in Figure 6. The best results have been achieved by applying a low-cost *pig tailed laser diode*, consisting of a laser diode coupled with a fiber. The laser diode can be positioned anywhere, even outside the cryostat.

In some applications, images from more than one light source are projected onto a single image sensor. This requires switching on the light sources alternatively, one after another. The laser diodes should then be externally powered. For C^3, so far, all light sources can operate continuously. Since the light power amplitude from a fiber tip is not critical, one high-power laser diode can act as input for a 16-channel splitter, all submerged in LN_2.

The single mode fiber tip should be well perpendicularly cleaved, polished and confined in a precision ferrule: these components are now widely available. The exiting beam has a perfect divergence such that it can be well pointed towards the zone lens.

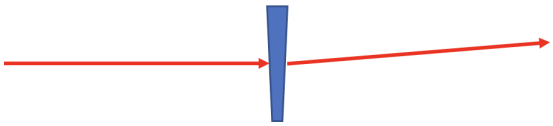

Figure 7: The effect of non planarity of a glass plate, causing a shift of the image position on the image sensor. An additional image shift occurs at the change of the index of refraction when filling the cryostat with LN_2. The large lever arm of order 0.5 m cause an image shift which is large with respect to the intrinsic spatial resolution of the applied Rasnik systems of 100 pm/$\sqrt{\text{Hz}}$.

(a)

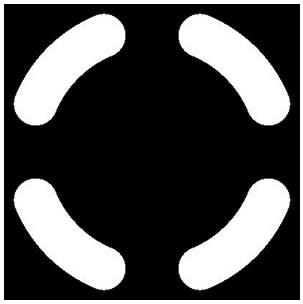

(b)

Figure 8: (a) Examples of micro-machined zone lens. (b) The 'four sausage' pattern of transparency of the zone lens.

2.2 Operating the zone lens in LN_2

So far, zone lenses were made in the form of a standard patterned chrome on glass substrate mask [7]. A glass plate, however, introduces an error (image displacement) due to non planarity as shown in Figure 7. This image shift changes again when LN_2 replaces ambient air. Due to the lever arm (0.5 m), the demand of planarity becomes unrealistic. As an alternative, the zone lens is milled out of a brass plate, see Figure 8a. This milling can be included in the process of making the Sticks (see Sect. 3). The pattern of the zone lens is shown in Figure 8b.

In this application, Rasnik measures only the *change of the position* of an image on the sensor, independent of the pattern of the image. There are, therefore, no stringent tolerances in the pattern of the zone lens (see Sec. 2.5).

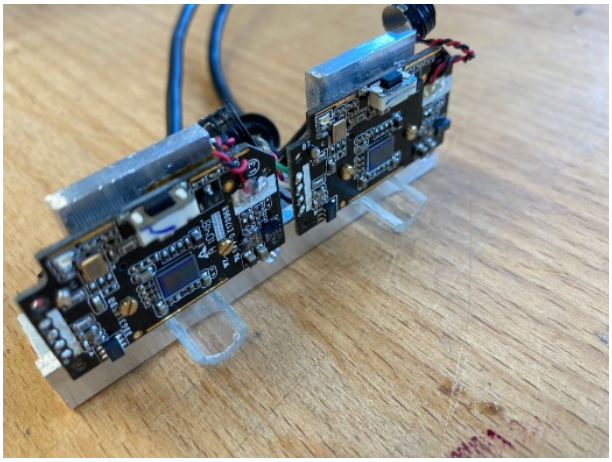

Figure 9: Two image sensor PCB's, subsequently called **cams**, mounted on a support plate. The image sensors were extracted from two Microsoft HD 3000 webcams, model 1456 (2010).

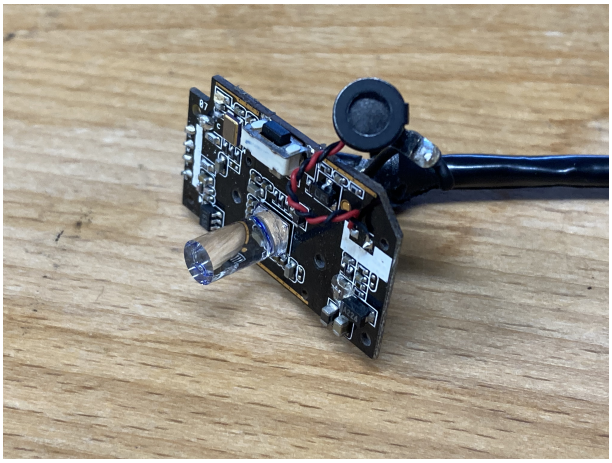

Figure 10: Image sensor with glued-on glass rod. The black cylinder is the webcam's microphone.

2.3 Operating the image sensor in LN_2

The Microsoft webcam HD-3000, commercially available in 2010, was tested successfully for operation in LN_2 [8], allthough its active area of 7 mm2 is rather small, and its maximum frame rate is only 7 Hz. The heat dissipation of 2.5 W by the image sensor card causes severe

bubble formation in LN_2. In addition, the warm pixel sensor will cause a density gradient in the nearby LN_2, causing a deflection of the incoming light beam. In a first attempt to reduce the disturbance due to bubbles passing the light beam path, 'cow catchers' were placed below the pixel sensor, as shown in Figure 9, with little effect. In a next attempt, a tube, rolled from a rectangular piece of Kapton foil, was placed against the surface of the pixel chip. Bubbles were growing inside the tube, and this attempt was discarded. Finally, a glass rod was glued onto the window of the pixel chip: see Figure 10, as was done with the laser diode shown in Figure 6. This method eliminates, in addition, the effect of a density gradient due to convection, in LN_2 near the warm surface of the pixel chip. The robustness, however, of the pixel chip assembly, in the environment of 80 K is not guaranteed. The development of a pixel image sensor with minimized power dissipation that could operate in LN_2 would ensure robust performance for operating in C^3.

2.4 Disturbances in the light path; beam shielding

There are two causes of disturbance in the optical path: bubbles, and local density fluctuations in LN_2. Bubbles could be caused by either dissipation of heat in a hot spot, or *nucleation* spots. The latter occurs, for instance, in a glass filled with sparkling water or beer. At micro-irregularities in the glass surface, bubbles grow, and leave the spot of creation due to buoyancy, eventually resulting in a chain of small bubbles.

The disturbing effect of bubbles can be eliminated by shielding the optical path as illustrated in Figure 11.

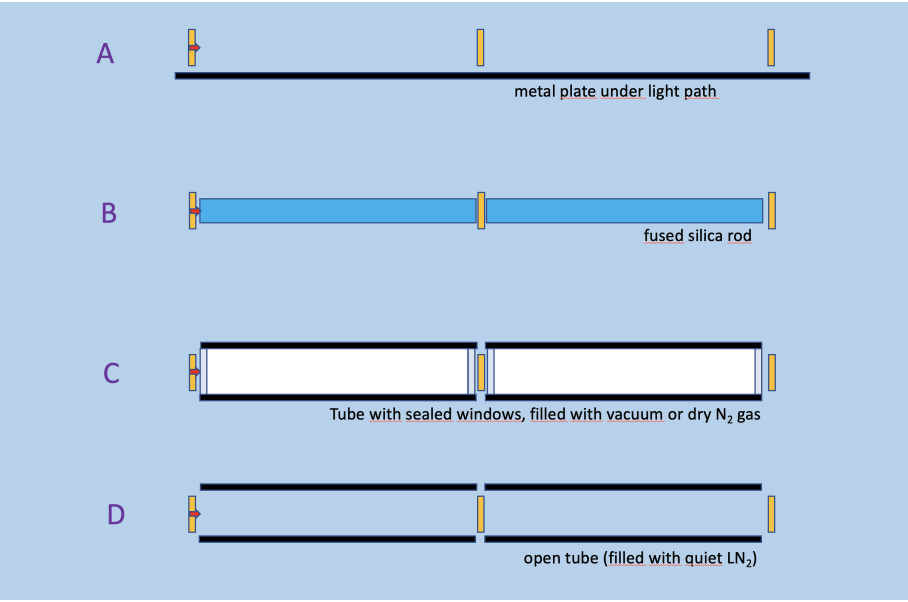

Figure 11: Several methods of beam shielding. The blue background of the figure represents LN_2 as medium.

A. Place a metal plate under the optical path. This stops bubbles from below, and reduces convection in the LN_2 above the plate. Bubbles, however, created by or close to the three Rasnik components, can still cause distortions, as well as bubbles formed at nucleation spots on the top side of the metal plate.

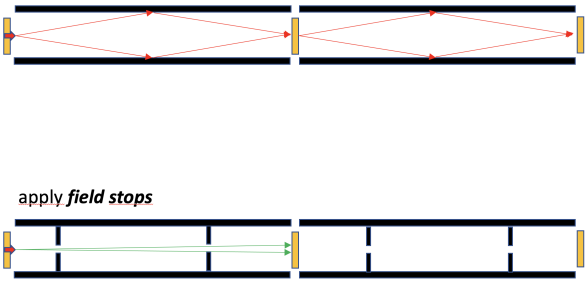

Figure 12: Suppression of reflection using field stops.

B. Replace the volume of the optical path by solid transparent material, i.e. glass, in the form of rods. Since the glass should stay free of the three Rasnik components, small volumes will be left unshielded. In practice, the transparency of glass rods is obstructed by non-homogeneity of the medium. The method is expected to work if fused silica is used. Another disadvantage is the tight tolerance in the perpendicularity to the optical axis of the rod's end planes, facing the zone lens.

C. This method has been demonstrated to work, but it is hard to guarantee that the vacuum, or pressure, is maintained over a period of years. In addition, the constraints in perpendicularity, and planarity of the windows facing the zone lens are hard to achieve when related to Rasnik's intrinsic precision of 5 nm/ $\sqrt{Hz}$.

D. Place open tubes such that the optical path is transversely confined. Bubbles from below are diverted around the optical path, and density fluctuations are strongly reduced due to the thermal conductivity of the tube. Due to the absence of material in the optical path, the direction of a light beam is not affected when changing the medium from vacuum to air or to LN_2. The inside of the tube should be free of nucleation spots. Another disturbing effect of containing the light beam in a tube is multiple reflection, shown in Figure12. This can be eliminated by placing diaphragms (field stops) as is indicated. In our set up, the (aluminium) tube and field stops were black anodised, reducing reflection, and leaving a smooth surface with little chance of having nucleation spots.

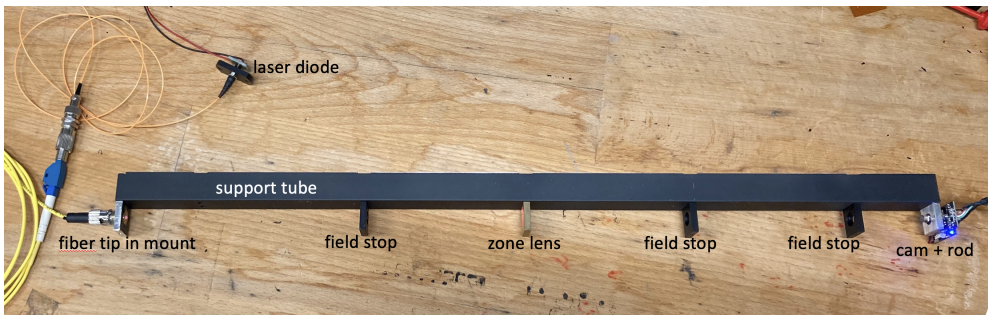

Figure 13: The test system.

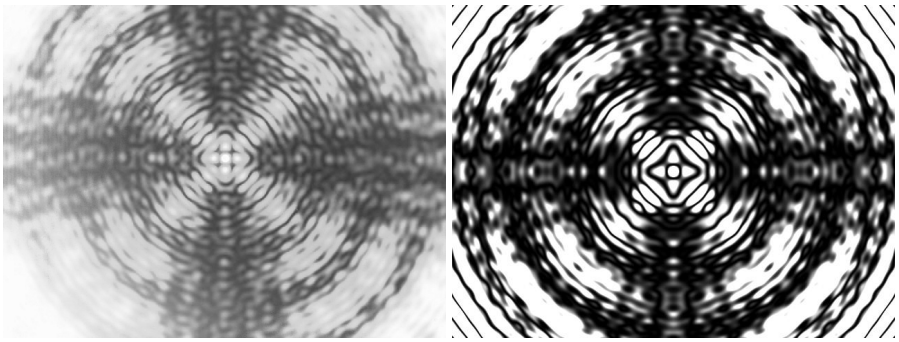

(a) (b)

Figure 14: (a) Image of the test system, taken in air. (b) Simulated image.

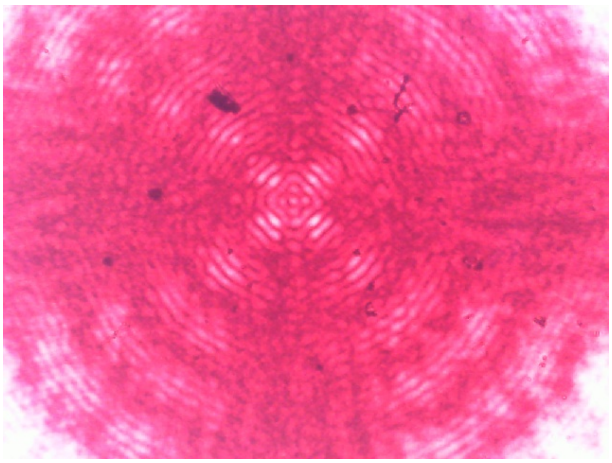

Figure 15: Image in LN_2. Note the change in the diffraction pattern due to the 20 percent shorter wavelength in LN_2. The stains in the image are due to dust particles sticking on the pixel chip.

2.5 Results

A test system, shown in Figure 13, was made using the following components:

- light source: Pigtail laser diode LD4B-639-FP-5-TH-3-MM6-FU-CW-1.0, equipped with a fiber jumper (give ID), ending in ferrule.
- zone lens: 'four sausage' pattern, with R_i = 0.96 mm, R_o = 1.36 mm, milled mechanically out of brass.
- the standard Microsoft HD-3000 image sensor, equipped with a glass rod diameter 5 mm, length 10 mm, glued on the window of the pixel chip, depicted in Figure 10.

The distance between the light source and the zone lens is 247.5 mm, and the distance between the zone lens and the pixel chip on the image sensor is 252.5 mm. Figure 14a shows an image taken in air, and a simulated image is shown in Figure 14b, demonstrating that the

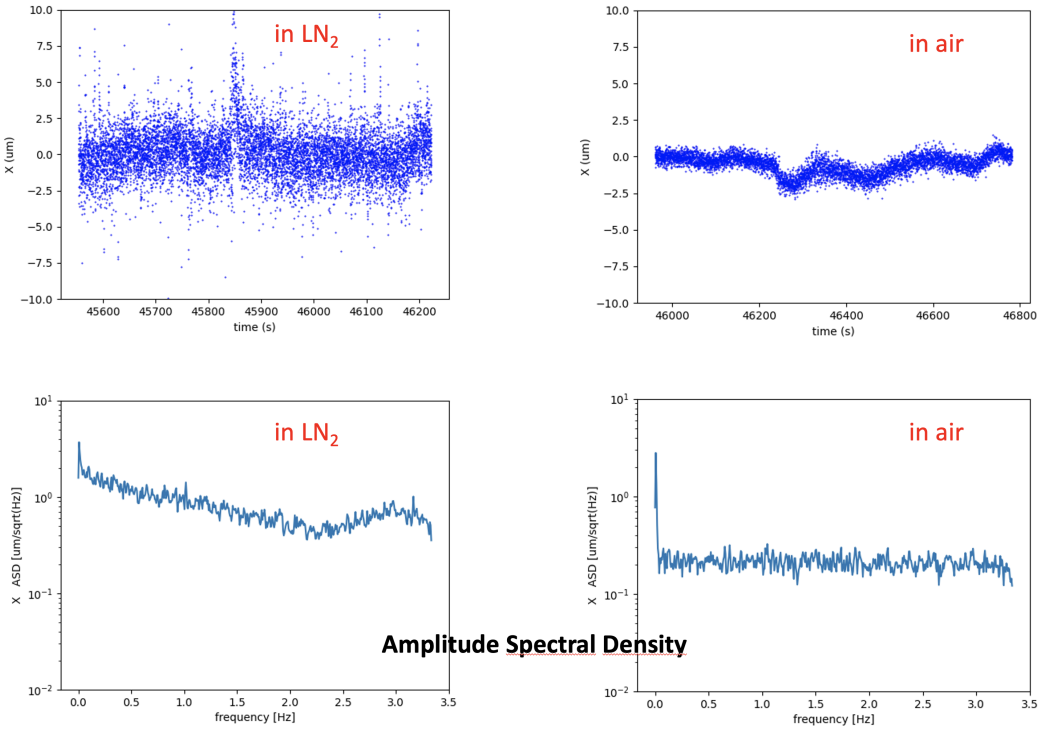

Figure 16: Results from the test system. Top right: raw X data, taken in air. Top left: raw X data taken submerged in LN_2. Bottom: ASD (Welch) plot of X data in air, and in LN_2, respectively.

diffraction process is well understood. The image is rich of black/white transitions favouring the spatial resolution of this Rasnik system [5]. Figure 15 is taken when immersed in LN_2. When displaying the video signals from the image sensor, instabilities are observed: the position of the diffraction pattern on the image sensor moves Brownian in the order of 50 μm RMS. In addition, image *deformation* is visible. This is due to bubbles, created at the 1.5 W dissipating image sensor, and to bubbles formed at *nucleation* spots. Possibly, deflections due to density fluctuations caused by convection play a role, but this can only be seen in absence of bubbles.

In the following, the data was taken before the fiber tip lightsource was applied, so the earlier laser diode was used.

The Rasnik output data is defined as the distance, in X and Y, between the position of the centre point of the diffraction pattern and the centre of the image pixel sensor.In Figure16, the X data is shown of the test system placed in air; the Y data looks identical. The X value of the first image is subtracted from the following values, thus eliminating the initial offset. The frame rate of the image sensor is 7 Hz. The noise level in air has a value of 0.2 μm/ $\sqrt{Hz}$, corresponding to a spatial resolution per image of 0.2 μm x $\sqrt{7Hz} = 0.5$ μm, in good agreement with earlier results [5]. In LN_2, a value in the order of 1 μm/ $\sqrt{7Hz}$ is reached: the effect of bubbles is clear. This is good enough for the alignment of the accelerator elements of C^3.

We conclude that Rasnik in LN_2 works adequately well, but for studying mechanical vibrations, the influence of bubbles should be greatly reduced.

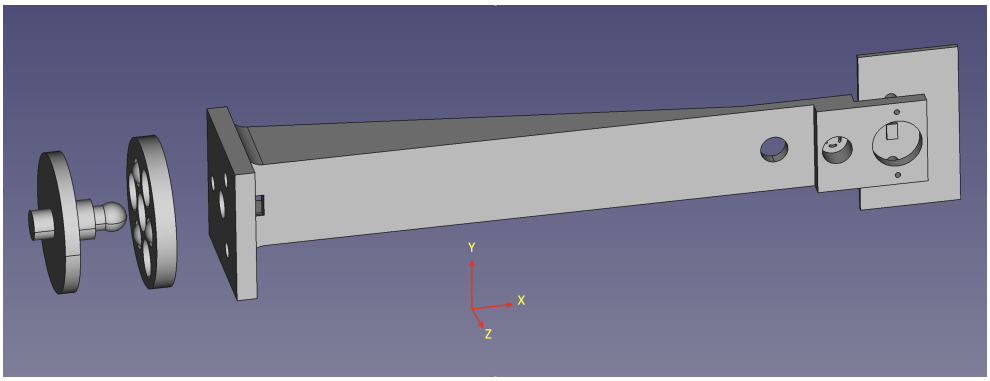

Figure 17: The stick, made from hardened steel. At left, the anchor is shown, to be mounted onto the Accelerator Structures and Quad. It is cold-press mounted in precision holes in the very soft copper Accelerator Structures and in the Quad. The (YZ) position of these precision holes is transferred to the spherical tip of the anchor which, in its turn, fits precisely in the hole in the base plate of the stick. The spacer, in the form of a disk holding three spheres, transfers the X position of local precision planes on Accelerator Structures and Quad to the base plane of the stick. The optical centres of image sensor, zone lens and light source are situated on the X-axis of rotation of the Stick, reducing the required precision in fixing its angle rotX.

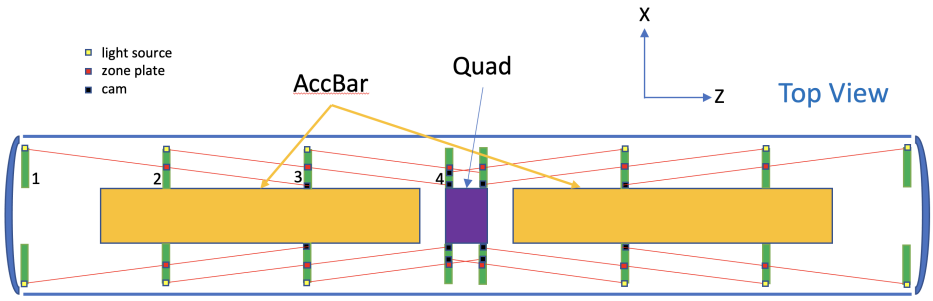

Figure 18: Layout of the Rasnik systems in the 3 m long Quarter Cryo Module QCM.

3 Rasnik systems for QCM

The Quarter Cryo Module QCM is the core of the ongoing R&D for C^3. It will also act as test facility for Rasnik systems, albeit that the Rasnik data is, at the same time, essential for the QCM tests to be carried out. In a first phase, the QCM will be loaded with dummy Accelerator Structures and a Quad module. The cryostat will be tested (vacuum, thermodynamics) and all mechanical aspects (suspension, actuators, stresses, deformation, vibrations)

will be measured. In a second phase, the Accelerator Structures and Quad will be replaced by operational ones, and the QCM will be tested as fully operational accelerator module.

3.1 The Accelerator Structure/Quad chains

The Rasniks for the QCM consist of two chains of 'standard' sticks, shown in Figure 17. The chains are placed at the +X and -X side of the Accelerator Structures and Quad, respectively, shown in Figure 18. Following the +X chain in this figure, going from left to right, sticks (labeled 1 - 4) are placed, respectively:

1. the endstick. This stick includes only a light source, and is mounted on the cryostat, without anchor and spacer.

2. standard stick mounted on Accelerator Structure, without image sensor.

3. standard stick, mounted on Accelerator Structure, complete.

4. standard stick, mounted on Accelerator Structure, without light source, and with addional image sensor, placed close to zone lens.

This pattern of four sticks is copied three times, forming, in symmetry, the two complete chains. The data from 12 Rasnik systems contains redundant values for five degrees of freedom of each of the two Accelerator Structures and the Quad. The less relevant mutual distance in Z is not measured.

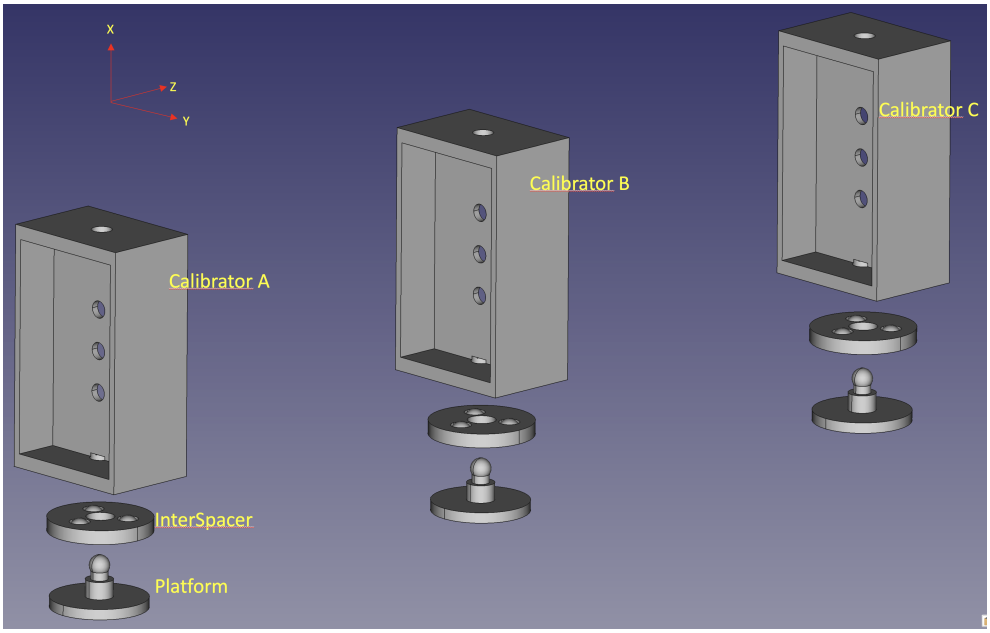

Figure 19: The calibration station.

3.2 The calibration of the Accelerator Structure/Quad sticks

Technically it is impossible to mount the light source, zone lens and image sensor with their optical centres, with micron precision, in nominal position, relative to the hole in, and the plane of the base plate of a stick. By means of a calibration procedure, the offsets of the optical centres can be obtained, providing corrections in raw data. With this, the alignment of the two Accelerator Structures and Quad is known, in 5D, after the sticks have been mounted correctly.

For this, a calibration station is made, consisting of three platforms, fixed on a granite table, shown in Figure 19. With simple means, the alignment of the three platforms can be better than 0.1 mm. The sagitta is defined as the distance, in X and Y, between the centre of the sphere of Platform B, and the line through the centres of the spheres of platforms A and C. The (vertical) X direction of the platforms should be correct within 10 μm rad, which can be obtained by rotating a spirit level around the X axis. Three identical calibrators are placed on top of the spacers, resting on the Platforms. The height of these calibrators is precisely equal, within 1 μm, and the top and bottom planes are plan-parallel within 10 μ rad. Calibrators A, B and C are equipped with a light source, zone lens and image sensor, respectively, forming a complete Rasnik system. The position of the diffraction pattern on the image sensor is registered. In a next step, all three calibrators are lifted from the InterSpacers, and rotated 180 deg around the Z axis, and placed back on the InterSpacers. Again, the position of the diffraction pattern on the image sensor is registered. It can easily be demonstrated that the shift of the diffraction pattern on the image sensor, before and after the rotation of the calibrators, equals 4 times the sagitta. Thus, after one rotation, the sagitta of the calibration station is known. Now, a set of three standard sticks, discussed in 3.1, can be placed on the calibration station. The X and Y data can be read out, and the X and Y offsets of this set can be obtained by applying a correction for the known sagitta. This procedure can be repeated for verification, and to obtain an estimation of the consistancy and precision. In the past, the precision was limited by the mechanical precision of the calibrators, reaching a level of 2 μm [9].

4 Conclusions and outlook

An image pixel sensor had been found which can operate in boiling liquid nitrogen at 80 K. With this, a Rasnik system has been constructed which operates in air as well as in liquid nitrogen, reaching a sagitta precision of 0.2 μm/ $\sqrt{Hz}$ and 1 μm/ $\sqrt{Hz}$, respectively.

The performance in liquid nitrogen is limited by bubbles passing the light path between light source and image pixel sensor. The performance is good enough to fulfill the requirements concerning alignment, but for studying the mechanical displacements (vibrations, deformations) of hot accelerator components, induced by bubbles, the formation of bubbles in the Rasnik area should be reduced. For this, a new ASIC image pixel sensor, LN_2 proof, should be developed. Its power dissipation should be minimized, it should have a large active area, and it should have frame rates up to 300 Hz, in order to measure vibrations up to 150 Hz [10]. The bubble disturbance can be further reduced using beam shielding elements deflecting the path of bubbles. The surface of shielding elements should be free of nucleation spots.

A design exists for chains of Rasniks in QCM. The sticks can fit well in the available space, and the optical path can be properly shielded.

5 Acknowledgments

We are grateful to neighbour Institute Amolf to provide us with LN_2. We thank Oscar van Petten for his excellent mechanical constructions, and Berend Munneke for applying his vacuum expertise. We are grateful for the help of Peter Jansweijer and Jan Willem Schmelling concerning optical fibers. We thank Robin Schmeitz for developing a method for micromachining small patterns using a large milling machine.

References

[1] Emilio Nanni et al.: *The C^3 Demonstration Research and Development Plan*, 2022 arXiv 2203.09076

[2] Stef M. J. Janssens: *Stabilisation and precision pointing quadrupole magnets in the Compact Linear Collider (CLIC)*, [Thesis, fully internal, Universiteit van Amsterdam]. http://hdl.handle.net/11245/2.154854

[3] M. Beker, G. Bobbink, B. Bouwens, N. Deelen, P. Duinker, J. van Eldik, N. de Gaay Fortman, R. van der Geer, H. van der Graaf, H. Groenstege, R. Hart, K. Hashemi, J. van Heijningen, M. Kea, J. Koopstra, X. Leijtens, F. Linde, J.A. Paradiso, H. Tolsma, and M. Woudstra. The Rasnik 3-point optical alignment system. *Journal of Instrumentation*, 14(08):P08010–P08010, aug 2019. DOI:10.1088/1748-0221/14/08/P08010

[4] H. van der Graaf et al.: *The ultimate performance of the Rasnik 3-point alignment system*, Nuclear Inst. and Methods in Physics Research, A 1050 (2023) 168160

[5] J.V. van Heijningen. Precision Improvement in Optical Alignment Systems for Linear Colliders. M.Sc. thesis, Nikhef, Amsterdam and Delft University of Technology, 2012

[6] H. Manaud Durand et al. Stretched wire offset measurements: 40 years of this technique at CERN. Presented at the 10th International Workshop on Accelerator Alignment, KEK, Tsukuba, Japan, 11–15 February 2008.

[7] Photronics. *1 Technology Dr, Bridgend CF31 3LU, United Kingdom.*

[8] K. Mavrokoridis, F. Ball, J. Carroll, M. Lazos, K. J. McCormick, N. A. Smith, C. Touramanis and J. Walker: Optical Readout of a Two Phase Liquid Argon TPC using CCD Camera and THGEMs, JINST 9 (2014) P02006

[9] H. van der Graaf: The calibration of the ATLAS muon spectrometer projective alignment systems ATL-MUON-2004-024, CERN, Geneva, Switzerland (2004).

[10] G. Ghibaudo and F. Balestra: Low Temperature Characterization of Silicon CMOS devices, Microelectron. Reliab. 37(1997) 9, 1353-1366.